



## Effect of plasticity on the measurement of residual stresses using ultrasound technique

R. Torkaman <sup>a</sup>, A.H. Mahmoudi <sup>a\*</sup>, M Ahmadi-Najafabadi <sup>b</sup>, A. Karbasian <sup>a</sup>

<sup>a</sup> Mechanical Engineering Department, Bu-Ali Sina University, Hamedan, Iran

<sup>b</sup> Mechanical Engineering Department, Amirkabir University of Technology, Tehran, Iran

### PAPER INFO

#### Paper history:

Received 14 July 2023

Received in revised form 4 August 2023

Accepted 5 August 2023

#### Keywords:

Ultrasound method

Residual stresses

Plasticity

Finite element analysis

Center-hole drilling

### ABSTRACT

Residual stresses can have detrimental effect on the life cycle of engineering components. They can also alter the accuracy of the fatigue life prediction models. Therefore, it is important to measure such stresses with accuracy. One of the issues with the destructive and semi-destructive methods of measuring residual stresses is the damage they cause in components. In the non-destructive ultrasonic method, not only does the piece remain intact, but it is also capable of measuring residual stresses even if there is no portability. There are different waves in the ultrasonic method for measuring residual stresses. In this study, longitudinal critically refracted (LCR) waves were used owing to their higher sensitivity, larger area they scan, and lower sensitivity to texture effect, which shows the preference of LCR waves to other waves. The purpose of this study was to investigate the effect of plasticity on the measurement of residual stresses by the ultrasonic method. With this end in view, three stainless steel disks were quenched at temperatures of 300 °C, 500 °C and 700 °C to induce different levels of residual stresses and subsequently different levels of plasticity. The properties of the piece were required for the numerical simulations and were obtained using the standard tensile test. The tensile test components were extracted from the initial sheet to measure the yield stress and modulus of elasticity. In order to measure the coefficient of acoustoelasticity, the tensile test specimens were applied to different stresses and the wave flight time was recorded; subsequently, using the slope of yield stress and the corresponding equations, the coefficient of acoustoelasticity was obtained for stainless steel 316L. Residual stresses were experimentally measured using the ultrasonic and center-hole drilling methods and the results were compared with those obtained from numerical analyses. Eventually, the results from center-hole drilling, ultrasonic method, and numerical simulation were compared and discussed. The measured residual stresses by the ultrasonic method illustrated a good compatibility with the center-hole drilling results in different disks and with three different quenching temperatures at 300°C, 500°C and 700°C.

## 1. INTRODUCTION

The use of ultrasonic waves to measure stress is being developed due to its non-destructiveness, portability, inexpensiveness, and not being limited to surface layers. Based on Murnaghan's theory of nonlinear elasticity [1], Huges and Kelly [2] managed to establish the theory of acoustoelasticity in 1953. They described the changes in the ultrasonic wave velocity as a function of elastic strains of the isotropic material. In 1958, the phenomenon of double refraction (or birefringence) of sound waves was discovered by Bergman and Shahbender [3] and Benson and Reelson [4]. In a tensile test sample, the velocity of the shear wave polarized along the applied stress axis was very different from the wave polarized perpendicular to the stress direction. This phenomenon was similar to the change in the speed of light in

a transparent object. Since the phenomenon of photoelasticity was previously used to determine the amount of stress, the ultrasonic birefringence capability was investigated and developed for stress analysis.

In 1988, Salamanca [5] was the first to use LCR waves to measure residual stresses caused by welding in steel. In 1995, Junghans and Bray [6] obtained the shape of the LCR wave field and the shear wave by placing a probe in the center of a semicircular piece and scanning the circumference of the circle with another probe. In 1991, Srinivasan et al. [7] used LCR waves to measure residual stresses in casting parts.

In 1967, Crecraft [8] showed that the acoustoelastic effect can be used to estimate the stress state in engineering parts. The velocity changes of ultrasonic waves caused by stress in steel samples were measured by Egle and Bray [9] in 1976. They published all five possible relative velocity changes in longitudinal and transverse waves under uniaxial stress and

confirmed the theoretical predictions. They concluded that LCR waves show the most sensitivity to stress changes.

In 2002, Dos Santos and Bray [10] made a comparison between stress measurement using shear waves and longitudinal waves. They used LCR shear waves and longitudinal waves to measure the stresses applied to a steel beam. The results were compared with the stresses obtained by dividing the applied force by the cross section of the beam. They observed that the longitudinal waves of LCR show more sensitivity to their stresses. In 2006, Jhang et al. [11] indicated that when a part is under mechanical load, the wave velocity in it changes and the acoustoelastic effect can be used to measure the existing stress.

In 2012, Albuquerque [12] used the ultrasonic method to determine the residual stress. In this uniaxial tension test, the sensitivity of the wave flight time was studied for several different waves in the applied stresses, the basis for calculating the coefficients was based on the relationship between stress changes and the change in the velocity of longitudinal and transverse waves in different directions .

For the first time, Salamanca [13] used longitudinal critical refraction waves or LCR waves for measuring residual stresses caused by welding in 60 series steel. Barry and Janghans [14] used LCR waves to measure residual stresses caused by welding in 60 series steel. They also measured the effect of temperature on the wave's time of flight. Tanala et al. [15] extracted the acoustoelastic coefficient of different types of ultrasonic waves for stainless steel 316L and aluminum alloy 5086. Tang and Barry [16] used LCR waves to measure stresses higher than the yield stress limit of 4140 steel and investigated the effect of plastic deformation on ultrasonic waves. Salamanca and Barry [17] used LCR waves to measure residual stresses caused by welding in heated and cold rolled sheets. They also investigated the effect of stress relief operations. Barry et al. [18] used LCR waves to measure the stress in the compressor and turbine rotor. Berry et al. [19] measured the residual stresses caused by aluminum rolling using LCR waves.

Acevedo et al. [20] tried to create an updated state of the art on acoustic waves NDT applied to AM metallic parts. Different measurement techniques were compared to ultrasonic waves non-destructive testing (UT) regarding both their capabilities and limitations. Zhan et al. [21] measured the residual stress in 7075 aluminum alloy FSW with laser ultrasonic technology. They used acoustoelastic constants to measure the longitudinal and transverse FSW residual stresses. Wang et al. [22] measured plane stress using an improved ultrasonic method. Based on the acoustoelastic theory, the expression between biaxial principal stresses and time of flight of LCR waves was deduced. They designed an ultrasonic wedge for generating LCR waves in the material under test. The value those measured by the ultrasonic method were then compared with DIC method and good agreement was observed. Liu et al. [23] derived the linear relation between TOF and stress based on acoustoelasticity effect. They

analyzed analytically influence of temperature variation and coupling condition on TOF .

In this paper, the residual stress resulting from the heat quenching treatment in disks quenched at 300 °C, 500 °C, and 700°C with a diameter of 100 mm and a thickness of 10 mm was measured in peripheral and radial modes by the center-hole drilling and ultrasonic methods and compared with numerical simulation. The stress and acoustoelastic coefficient were extracted by examining the peripheral and radial wave velocities in different quenched states at different temperatures. The development of acoustoelastic coincided with the interest in estimating third-order elastic coefficients

## 2. ULTRASONIC THEORY

The ultrasonic method is evaluated for measuring stress based on the dependency of acoustic wave speed upon the elastic strain in a material, which is known as acoustoelasticity. The nature of acoustoelasticity depends on the material and the type of propagating wave. Figure 1 shows components of a beam under stress in which waves propagate in three different directions perpendicular to each other. The first index of the velocities indicates the direction of wave propagation and the second one is for the direction of the particle motion. In Fig. 1a, the wave propagates parallel to the loading direction and V11 is the particle velocity in the same longitudinal wave direction. V12 and V13 indicate the velocity in the vertical plane (shear wave). The most striking changes in the time of wave flight due to strain are related to longitudinal waves, then to shear waves. Other waves do not show significant sensitivity to deformation. Regarding Figure 1, Hugh and Kelli [2] obtained the equations related to the relationship between ultrasonic wave velocities and elastic strain in an isotropic material as Equations (1) to (3).

$\rho_0 V_{11}^2 = \lambda + 2\mu + (2L + \lambda)\theta + (4m + 4\lambda + 10\mu)\alpha_1$	(1)
$\rho_0 V_{22}^2 = \lambda + 2\mu + (2L + \lambda)\theta + (4m + 4\lambda + 10\mu)\alpha_2$	(2)
$\rho_0 V_{33}^2 = \lambda + 2\mu + (2L + \lambda)\theta + (4m + 4\lambda + 10\mu)\alpha_3$	(3)

Where  $\alpha_1$  ,  $\alpha_2$ , and  $\alpha_3$  are principal strains,  $\rho_0$  is the density,  $\mu$  and  $\lambda$  are second-order elastic constants (Lamé's constants), L and m are third-order elastic constants,  $V_{ij}$  is wave velocities in i direction and particle vibrations in j direction. In longitudinal waves, the direction of propagation is along the same direction as the vibration; consequently,  $V_{11}$ ,  $V_{22}$ , and  $V_{33}$  indicate longitudinal waves.  $V_{11}$  is the velocity of the longitudinal wave that propagates along direction 1. The other velocities are for transverse waves in which the particles vibrate perpendicular to the wave propagation. Using the obtained values and substituting them in the relations, Equation 1 is expressed as Equation 4.

$\rho_0 V_{11}^2 = \lambda + 2\mu + [4(\lambda + 2\mu) + 2(\mu + 2m) + \nu\mu \left(1 + \frac{2\nu}{\lambda}\right)]\epsilon$	(4)
---	-----

For calculating velocity variation with respect to strain, it is sufficient to differentiate Equation 4 by strain. Thus, Equation 5 is obtained where  $L_{11}$  is the acoustoelastic constant for the

LCR waves.

$$\frac{dV_{11}/V_{11}^0}{d\varepsilon} = 2 + \frac{\mu+2m+\mu+\vartheta(1+2l/\gamma)}{\gamma+2\mu} = L_{11} \quad (5)$$

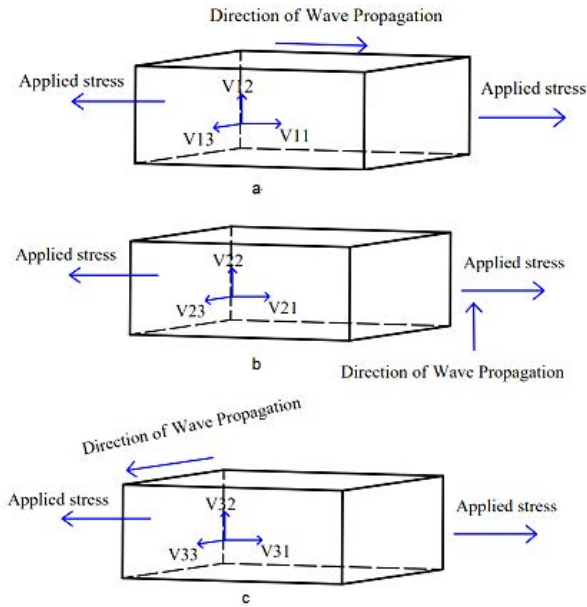


Figure 1. Plane wave velocity and stress field

3. RESEARCH METHOD

This study was aimed to investigate the effect of plasticity on measuring residual stresses using the ultrasonic method. To this end in view, three disks were quenched at 300 °C, 500°C, and 700 °C; subsequently, the residual stresses were measured using the incremental center-hole drilling (ICHD) method and then the results were compared with those obtained by ultrasonic method and numerical simulation. Being heated respectively to 300 °C, 500°C, and 700 °C, the material was uniformly sprayed with water so as to reach the ambient temperature. After creating residual stresses using the quenching method, the stresses were measured by the ultrasonic method inside the water container. It was done as stated above due to advantages of measuring stresses in the water over doing that using the Plexiglas method, including removing Plexiglas so the wave passes through less material, which is the most tangible benefit of this method. The specimen were made of steel 316L, and its properties were obtained after conducting the tensile test on the specimens before quenching, which are shown in Figure 2. Table 1 shows the material properties obtained from the tensile test and Table 2 presents the chemical composition of the used material.

In order to measure the wave velocity, the ultrasonic device, made by Optel, was used with its frequency ranging from 0.5 to 25 MHz and accuracy of 10 nanoseconds. Three probes were used, one of which was a transmitter and the other two were receivers with a frequency of 4 MHz which is suitable for 1mm penetration beneath the surface. The 10mm diameter probe is displayed in Figure 3.

3.1. DESIGNING A PROBE HOLDER

To set probe angles, a holder was required to fix the transmitter and receiver in a specific position for sending waves, which can move in the longitudinal direction so the distance between probes can be changed. A view of the designed holder is shown in Figure 4.

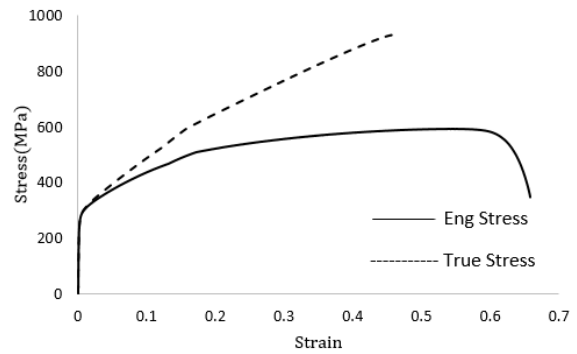


Figure 2. Engineering and true stress-strain of 316L steel before quenching

Table 1. Properties of steel 316L obtained from the tensile test before quenching

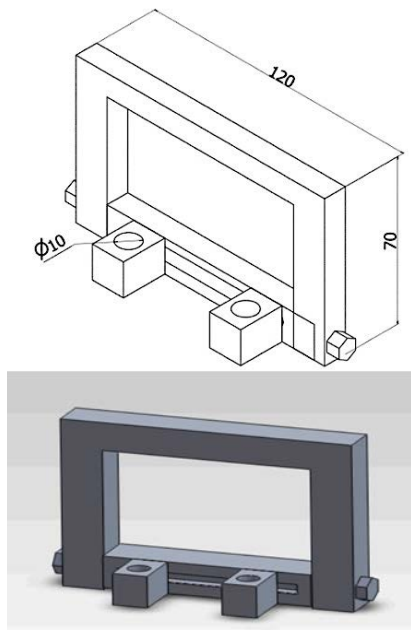
Properties	Value	Standard Deviation
Yield stress (MPa)	255	5.4
Modulus of elasticity (GPa)	216	2.05
Ultimate tensile strength (MPa)	591	4.64

Table 2. Chemical composition of 316L

Fe	C	Si	Mn	P	S	Cr	Mo
Base	0.024	0.41	1.79	0.020	0.013	16.95	2.034
Ni	Al	Co	Cu	Nb	Ti	V	W
10.06	0.004	0.41	0.41	0.008	0.002	0.053	0.077



Figure 3. Specifications of the 5MHz probe



**Figure 4.** A view of the designed probe holder (dimension in mm)

### 3.2. APPLYING THE LCR WAVE

When a longitudinal wave hits the intersection of two materials with different impedances with an oblique angle, a wave transformation occurs. As it is shown in Figure 5, a part of it turns to the transverse component both in reflection and refraction. The diffraction angles of the longitudinal and transverse components of the wave in the second medium ( $\theta_s, \theta_1$ ) are related to the radiation angle ( $\theta_0$ ). The relationship between these angles is based on Snell's law, which is expressed as Equation 6.

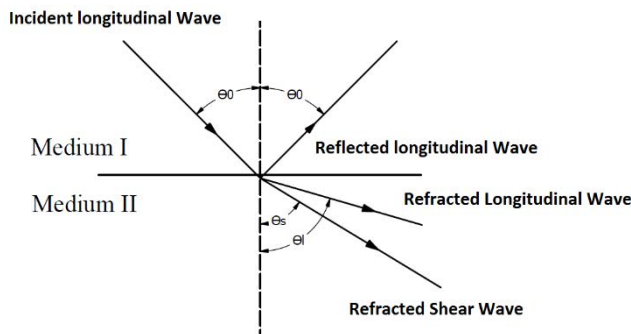


**Figure 5.** Wave diffraction in the intersection of two

$$\frac{\sin \theta_0}{C_0} = \frac{\sin \theta_1}{C_1} = \frac{\sin \theta_s}{C_s} \quad (6)$$

In equation 6,  $C_0$  and  $C_1$  are the longitudinal wave velocities in the first and second environments, respectively, and  $C_s$  shows the shear wave velocity in the second environment. According to the above equation and measuring the ultrasonic wave velocity in water and steel, the angle can be obtained as shown in Figure 6 and 7.

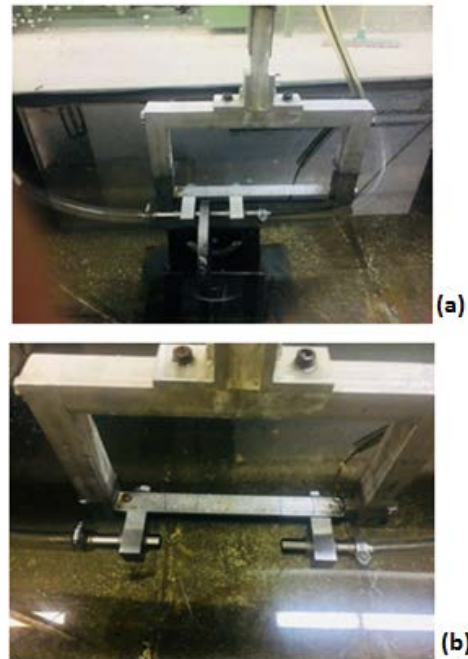


**Figure 6.** Measurement of wave velocity in (a) steel 316L and (b) water

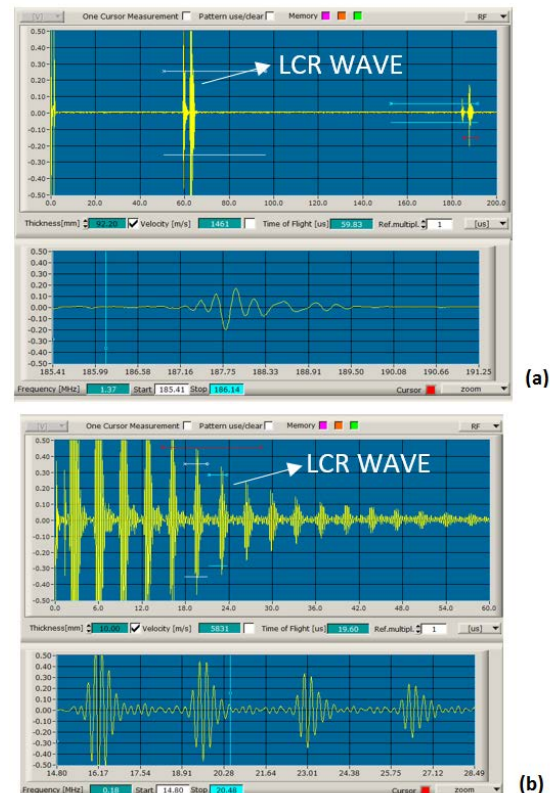


**Figure 7.** Method of measuring the obtained velocity in (a) steel 316L and (b) water

After measuring the velocities in water and steel, the angle was calculated and its value was 14.51°.



### 3.3. MEASURING THE ACOUSTOELASTIC COEFFICIENT

In order to obtain stresses in a piece, the acoustoelastic coefficient is required, which can be obtained by performing the tensile test. To obtain this coefficient, an ultrasonic device, tensile test apparatus, probe, couplant, and Plexiglas machined with laser are required. The way it works is that the test specimen, prepared according to ASTM-8M, is inserted into the tensile test device between two jaws and then the probes are impregnated with a couplant and placed in the Plexiglas. A screw is designed for each probe so that the force and thickness of the couplant remain constant during the experiment. The Plexiglas is mounted on the tensile test specimen using a clamp, so that the thickness of the couplant between the Plexiglas and the specimen remains constant during the test; subsequently, the tension is applied to the specimen and as it is under tension, the wave flight time is recorded by one transmitter probe and two receiver probes. In this study, the specimen was subjected to four stresses of 50, 100, 150, and 200 MPa, respectively, and the wave flight time was recorded. Then, Equation 7 can be used to obtain the acoustoelastic coefficient.

$$\sigma_y = \frac{E\{t - t_0\}}{L_{11} * t_0} \quad (7)$$

In equation 7,  $\sigma_y$  is the yield stress,  $E$  is Young's modulus.  $L_{11}$ ,  $t$  and  $t_0$  respectively are the acoustoelastic coefficient, time of flight (TOF), and time of flight in stress-free specimen. In the above equation,  $\sigma_y$  is extracted from the tensile test; therefore, Equation 7 could change to Equation 8 and  $L_{11}$ , the acoustoelastic coefficient, is calculated from the following equation.

$$L_{11} = \frac{E(t - t_0)}{\sigma_y * t_0} \quad (8)$$

It is then possible to calculate  $E(t-t_0)/t_0$  with respect to the wave flight time recorded at the specified stress and obtain the acoustoelastic coefficient from the slope of  $\sigma_y$  and  $E(t-t_0)/t_0$ . A view of the measurement and the diagram obtained is shown in Figures 8 and 9.



Figure 8. A view of measuring the acoustoelastic coefficient for steel 316L

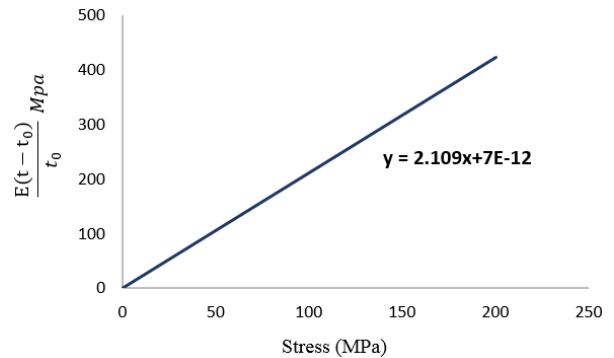


Figure 9. Diagram obtained for the steel 316L elasticity coefficient

### 4. PERFORMING CENTER-HOLE DRILLING TO COMPARE AND VALIDATE THE EXPERIMENT

Center-hole drilling is a common method and the first method of measuring residual stresses. Its popularity is due to its easy application, low damage to the specimen, and high reliability. In this method, a shallow hole with a depth almost equal to the diameter of the hole is created inside the specimen, so the released stresses are measured by a set of strain gauges in a specific formation known as rosette. Special precautions are taken into account during drilling (such as preparing the surface for strain gauge installation, etc.). In this method, after penetrating the place using a drill or milling machine, the released stresses are determined using the mounted rosette; consequently, the initial residual stresses are measured using elasticity equations. In most cases, center-hole drilling and a set of strain gauges are used when the stress field is uniform in the depth of the hole. In such conditions, coefficients of the experimental calibration can be used to calculate the residual stresses. Figure 10 indicates an overview of the residual stress measurement by the center-hole drilling method. The tool diameter was 1.8mm and the depth of hole drilling was 1.5mm.

### 5. NUMERICAL ANALYSES

In this study, since it does not deal with the dynamic finite element problem, the standard Abaqus mode was used for the quench simulation. The problem here is the analysis of uncoupled heat transfer with stress analysis, which deals with heat transfer analysis first, regardless of the stresses or displacements. Heat transfer is of the type of conduction, forced convection, and radiation, and the temperature at each node will be the software output parameter. Then, in another stress analysis, the temperature history obtained for each node is used as the input and then the displacements and subsequently the stresses and strains are extracted. The material properties are employed based on the data obtained from the experiments for steel 316L and the results of equivalent plastic strain and plasticity caused by the heat quenching treatment are given in Figures 11 and 12 for the simulated disks. The element type was C3D8R and the converged mesh size in the FE simulations was 0.5 mm.

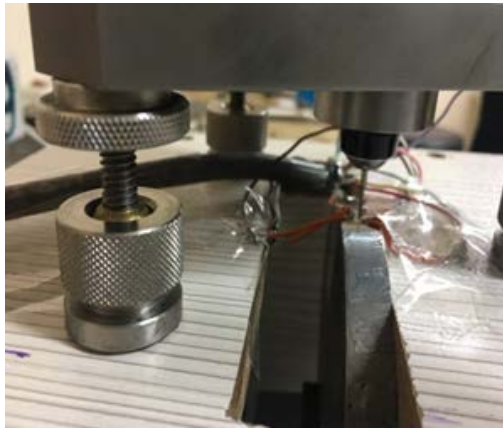


Figure 10. Center-hole drilling method

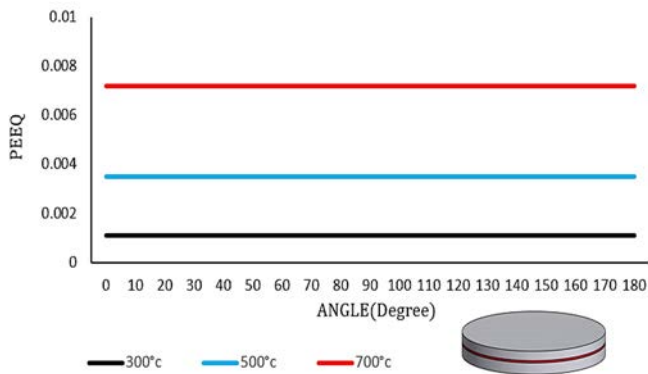


Figure 11. The value of equivalent plastic strain in the specific path

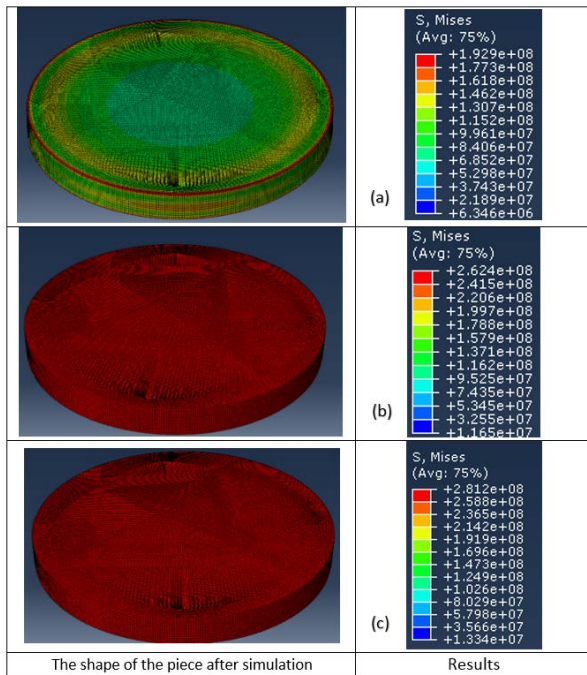


Figure 12. Von Mises Stress distribution for the quenched disks at a) 300 ° C b) 500 ° C, c) 700 ° C

## 6. RESULTS AND DISCUSSIONS

Results for the quenched disks at 300 °C and 700 °C are shown in Figure 13. As it is seen, there are no plasticity in the disk with 300°C quenching temperature; consequently, there are a good agreement between the numerical simulation, Incremental center hole measurement and ultrasonic method in both 700°C and 300°C. Also, the results for the disk quenched at 500 °C are shown in Fig. 13 as can be seen, the result of FE and ultrasonic had a suitable compatibility in 500°C quenched disk. the effect of plasticity is evident in 500 °C and 700 °C quenched disks.

### 6.1. THE EFFECT OF PLASTICITY

In the previous section, the values of residual stresses in the quenched disks were compared using numerical simulation and two experimental methods.

As can be seen, the results in the disk quenched at 300 °C were measured by both ultrasonic and ICHD methods with acceptable error. There is no plasticity seen in the disk quenched at 300 °C; however, the ultrasonic method is in good agreement with center-hole drilling and numerical simulation.

There is also a good agreement between the ultrasonic method and the numerical simulation in the sample quenched at 500 °C. As can be seen, in the quenched sample, taking into account the difference in the residual stresses obtained from both laboratory methods, the error value is lower than the disk quenched at 300 °C.

In the disk quenched at 700 °C, the plasticity increases, and it is reasonable to observe this rise in the plasticity as the temperature increases. In the disk quenched at 700 °C, there is a good agreement between the results obtained from center-hole drilling, the ultrasonic method, and numerical simulation.

In order to investigate the effect of plasticity, the values of error in the three disks were extracted based on the FE results. The results are shown in Table 3, where center-hole drilling and the ultrasonic method are compared.

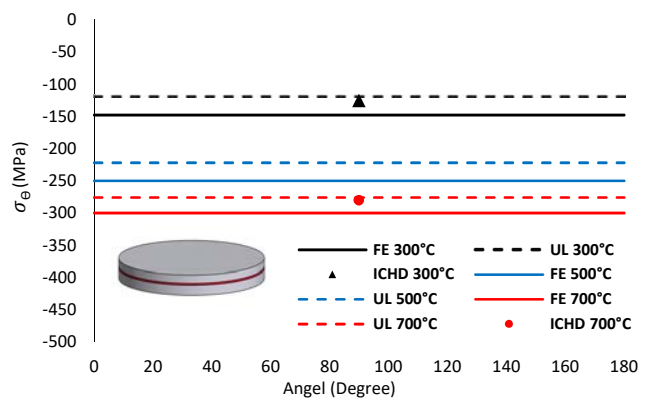


Figure 13. Hoop stress at the surface of the disc quenched at 300 ° C, 500°C, and 700°C

**Table 3.** The values of error in plasticity

Sample	Error in ultrasonic method	Error in center-hole drilling method
300 °C – heat treatment	19.6%	14.9%
500 °C – heat treatment	11.2%	-
700 °C – heat treatment	8%	7%

According to the results, the experimental methods (namely, incremental center-hole drilling and ultrasonic method) had a good agreement with numerical simulation. It is evident in Figure 13 the values of residual stresses resulting from the quenching were measured with acceptable accuracy by the ultrasonic method. The reason for using the incremental center-hole drilling method to validate the results was that it can measure the residual stresses for 1mm to 1.5mm beneath the surface similar to the resolution of the ultrasound probe. Regarding all the obtained results, it can be concluded that with increasing the plasticity, the errors were decreased. This phenomenon, based on the measured values, can be stated in this way that the values of stresses have a greater difference with the increase in plasticity in disks quenched at 300 °C, 500 °C, and 700 °C, respectively, and the decrease in the error is due to the high stress levels. It should be regarded that the ultrasonic method, for studying plasticity in measuring residual stresses, works based on variation in wave velocity when there is a change in the material's structure; consequently, this method has lower accuracy in measuring residual stresses. As can be seen, the temperature increases, the values of the residual stresses become closer and the level of residual stresses in the laboratory state is definitely not the same, and there is a difference, causing a non-uniform movement of wave and changes in the wave velocity. This effect can be attributed to the influence of plasticity on ultrasonic waves, so as observed, the value of difference in the measured stresses increases with increasing stress. It can be concluded that the ultrasonic method can be used as a non-destructive method of measuring residual stresses. This method, unlike other methods of measuring residual stresses, is less costly. In the experimental methods, an attempt was made to perform it in an ideal way. For modeling the specimens, the tensile test was performed and actual specifications of specimens under the tensile test were used for simulation; however, this method, similar to all methods, is not error-free.

## 7. CONCLUSION AND ERROR INVESTIGATION

In this paper, the proposed ultrasonic method was employed to measure the residual stresses in the quenched Disks. The effectiveness of the method was verified by comparing it with ICHD method and FE analysis results. Briefly, it could be concluded:

1. The proposed ultrasonic method was practical to measure the residual stresses and the results showed good agreement with ICHD and FE results.
2. Ultrasonic waves scan a volume of the material as they travel from the transmitter probe to the receiver probe. The

measured flight time is actually the average time during which the wave flies through the material. Therefore, it can be concluded that the measured residual stresses are the average residual stresses in the material between the two receiver probes. The longer the distance of the probes, the greater the distance travelled by the wave and the greater the error. Such errors are an inherent part of using ultrasonic waves.

3. The larger the probe diameter is, the greater the error becomes. In this case, the gain of the LCR wave must be increased in order to detect the echo of the LCR, which reduces the reproducibility. This factor is also an inherent error of ultrasonic waves.
4. By doubling the distance between the receiver probes, the wave flight time doubles as well, and by constant resolution at the time of flight reading, the resolution of the stress measurement is halved. The larger the distance between the receiver probes, the more accurate the stress measurement will be. Unfortunately, in this study, due to the small size of the components, it was not possible to increase the distance beyond the specified value.
5. By quenching operation, the microstructure of the component undergoes changes; thus, wave velocity is affected.
6. Temperature changes in the component cause the error.
7. Quenching components and the amount of water sprayed are definitely uniform, which causes error.
8. Cutting and machining the components is not stress-free since they have a small amount of residual stresses that cannot be measured and it causes errors.

## 9. REFERENCES

1. F. D. Murnaghan, Finite Deformation of an Elastic Solid, Wiley, New York, 1951.
1. D. S. Hughes, J. L. Kelly, Second Order Elastic Deformation of Solids, Physical Review 92 (1953) 1145-1149, <https://doi.org/10.1103/PhysRev.92.1145>
1. R. M. Bergman, R. A. Shahbender, Effect of Statically Applied Stresses on the Velocity of Propagation of Ultrasonic Waves, J. Appl. Phys. 29 (1958) 1736-1738, <https://doi.org/10.1063/1.1723035>
1. R. W. Benson, V. J. Realsen, Acoustoelasticity, Prod. Eng. 30 (1959) 56-59.
1. T. Leon-Salamanca, D. E. Bray, Residual Stress Measurements in Steel Plates and Welds Using Critically Refracted (LCR) Waves, Research in Nondestructive Evaluation 7 (1995) 169-184, <https://doi.org/10.1007/BF01606385>
1. P. Junghans, D. E. Bray, Beam Characteristics of High Angle Longitudinal Wave Probes NDE: Applications, Advanced Method, and codes and Standards, Proceedings ASME Pressure Vessels and Piping Conference, 9 (1991) 23-27

7. I. M. Srinivasan, D. E. Bray, P. Junghans, A. Alagarsamy, Critically Refracted Longitudinal Waves Technique: A New Tool for the Measurement of Residual Stresses in Castings, AFS (American Foundrymen Society) 91 (1991)
8. I. D. I. Crecraft, The Measurement of Applied and Residual Stresses In Metals Using Ultrasonic Waves, J. Sound vid. 5 (1967) 173-192, [https://doi.org/10.1016/0022-460X\(67\)90186-1](https://doi.org/10.1016/0022-460X(67)90186-1)
9. I. D. M. Egle, D. E. Bray, Measurement of Acoustoelastic and Third Order Elastic Constants for Rail Steel, J. Acoust. Soc. Am. 60 (1976) 741–744, <https://doi.org/10.1121/1.381146>.
10. I. A. A. D. Santos, D. E. Bray, Comparison of Acoustoelastic Methods to Evaluate Stresses in steel Plates and Bars, Journal of Pressure Vessel Technology 124 (2002), 354-358, <https://doi.org/10.1115/1.1484114>
11. K. Jhang, H. Quan, J. Ha, N. Kim 2006, Estimation of clamping force in high-tension bolts through ultrasonic velocity measurement, Ultrasonics 44 (2006) 1339-1342. <https://doi.org/10.1016/j.ultras.2006.05.190>.
12. V. Albuquerque, C. Silva, P. Normando, E. Moura, J. Tavares, Thermal aging effects on the microstructure of Nb-bearing nickel-based superalloy weld overlays using ultrasound techniques, Materials & Design 36 (2012) 337-347. <https://doi.org/10.1016/j.matdes.2011.11.035>
13. I. T. Leon-Salamanca, Ultrasonic Measurement of residual stress in steels using Critically Refracted Longitudinal Waves (Ler), Texas A & M University, Department of Mechanical Engineering (1988).
14. I. D. E. Bray, P. G. Junghans, Applications of the LCR Ultrasonic Technique for Evaluation of Post-Weld Heat Treatment in Steel Plates, NDT&E International, 28 (1995) 235-242, [https://doi.org/10.1016/0963-8695\(95\)00020-X](https://doi.org/10.1016/0963-8695(95)00020-X).
15. I. E. Tanala, G. Bourse, M. Fremiot, J. F. De Belleval, Determination of near surface residual stresses on welded joints using ultrasonic methods, NDT&E International 28 (1995) 83-88, [https://doi.org/10.1016/0963-8695\(94\)00013-A](https://doi.org/10.1016/0963-8695(94)00013-A).
16. I. W. Tang, D. E. Bray, Stress and Yielding Studies Using Critically Refracted Longitudinal Waves, American Society of Mechanical Engineers, Pressure Vessels and Piping Division (Publication) PVP, 322 (1996) 41-48.
17. I. T. Leon-Salamanca, D. E. Bray Residual Stress Measurements in Steel Plates and Welds Using Critically Refracted (LCR) Waves. Research in Nondestructive Evaluation, 7 (1996) 169–184, <https://doi.org/10.1007/BF01606385>
18. I. D. E. Bray, W. Tang, D. Grewal, Ultrasonic Stress Evaluation in a Turbine/Compressor Rotor. Journal of Testing and Evaluation, 25 (1997), <https://doi.org/10.1520/JTE11361J>.
19. I. D. E. Bray, S-J. KIM, M. Fernandes, Ultrasonic Evaluation of Residual Stresses in Rolled Aluminum Plates, American Institute of Physics 497 (1999), 443-448, <https://doi.org/10.1063/1.1303086>
20. I. R. Acevedo, P. Sedlak, R. Kolman, M. Fredel, Residual stress analysis of additive manufacturing of metallic parts using ultrasonic waves: State of the art review, Journal of Materials Research and Technology 9 (2020) 9457-9477, <https://doi.org/10.1016/j.jmrt.2020.05.092>
21. I. Y. Zhan, Y. Li, E. Zhang, Y. GE, C. Liu, Laser ultrasonic technology for residual stress measurement of 7075 aluminum alloy friction stir welding, Applied Acoustics 145 (2019) 52-59, <https://doi.org/10.1016/j.apacoust.2018.09.010>.
22. I. W. Wang, C. Xu, Y. Zhang, Y. Zhou, S. Meng, Y. Deng, An improved ultrasonic method for plane stress measurement using critically refracted longitudinal waves, NDT & E International 99 (2018) 117-122, <https://doi.org/10.1016/j.ndteint.2018.07.006>
23. I. H. Liu, Y. Li, T. Li, X. Zhang, X. Zhang, Y. Liu, K. Liu, Y. Wang, Influence factors analysis and accuracy improvement for stress measurement using ultrasonic longitudinal critically refracted (LCR) wave, Applied Acoustics 141 (2018) 178-187, <https://doi.org/10.1016/j.apacoust.2018.07.017>.